Applied Physics Letters ARTICLE scitation.org/journal/apl

Analysis of the improved thermal stability of Al-doped ZnO-adopted organic solar cells

Cite as: Appl. Phys. Lett. **118**, 023302 (2021); doi: 10.1063/5.0032729
Submitted: 10 October 2020 · Accepted: 24 December 2020 ·
Published Online: 15 January 2021

Jaehoon Kim,[1,a)] Yeonkyung Lee,[1] Jun Young Kim,[2] Hyung-Jun Song,[3] Jiyun Song,[1] Hyunho Lee,[4] and Changhee Lee[1,a)]

AFFILIATIONS

[1]Department of Electrical and Computer Engineering, Inter-University Semiconductor Research Center, Seoul National University, Seoul 08826, South Korea
[2]Department of Semiconductor Engineering, Engineering Research Institute (ERI), Gyeongsang National University, 501 Jinjudaero, Jinju, Gyeongnam 52828, South Korea
[3]Department of Safety Engineering, Seoul National University of Science and Technology, Seoul 01811, South Korea
[4]Department of Electronic Engineering, Kwangwoon University, 20 Kwangwoon-ro, Nowon-gu, Seoul 01897, South Korea

[a)]**Authors to whom correspondence should be addressed:** jplane@snu.ac.kr and chlee7@snu.ac.kr

ABSTRACT

The stable performance of organic solar cells (OSCs) at high temperatures is a critical issue for their commercialization. Although a few studies have reported the improved stability of OSCs that adopted Al-doped ZnO (AZO) as an electron transport layer (ETL), systematic research that validates the origins of this improvement has been lacking. In this work, we investigated the underlying mechanism for the improved stability of an OSC with AZO. By adopting AZO, the power conversion efficiency reached 8.65% and retained 70% of its initial value at 85 °C for 6 h, which was an increase in stability of 46% compared to that of an OSC with pristine ZnO. We found that the improved stability of the OSC with AZO originated from the decrease in oxygen defects and the space-charge limited current region through trap-related analyses and the Mott-Gurney law. Therefore, the results supported the enhanced thermal stability of OSCs that incorporated AZO as an ETL.

In response to the global demand for environmentally friendly energy sources,[1] tremendous effort has been made to develop efficient and stable solar cells. In particular, organic solar cells (OSCs) have been increasingly studied owing to their low-cost fabrication,[2,3] flexibility,[4,5] and a wide range of applicability.[6,7] However, mass production has been delayed because of the relatively low power conversion efficiency (PCE) and intrinsically low stability of OSCs. Although the low PCE has been comparatively resolved through various approaches,[8–10] the OSC is still vulnerable to harsh outdoor conditions.[11,12] Since the working principle of organic materials is based on conjugated π-bonds, these organic materials are easily deteriorated by external conditions, such as the presence of oxygen and the levels of humidity, light, and heat.[12] Furthermore, since the representative structures of OSCs are mostly based on bulk heterojunctions (BHJs),[13] thermal stress easily leads to phase separation inside the BHJ active layer.[14–16] Thus, a number of approaches have been reported to reduce the severe thermal degradation of OSCs.

The guiding articles can be categorized based on the synthesis of stable donors or nonfullerene acceptors,[17–19] additive engineering,[20–22] structural modification,[23–25] and interfacial engineering.[26–29] Among these methods, the modification of interfacial layers seems to be the most attractive since it is simple and widely applicable. In particular, several articles highly evaluated Al-doped ZnO (AZO) due to its high efficiency and stability.[29–32] However, most studies focused on the decrease in photoinduced degradation, where the reasons for improvement were attributed to the facilitated electron extraction,[30] alteration of the work function,[31] and reduced oxygen chemisorption.[32] Despite progress in recent studies, an exhaustive and systematic study that clearly validates the origin of the improved thermal stability has been lacking.

This work demonstrates that adopting AZO as an electron transport layer (ETL) significantly increased the thermal stability at 85 °C. Although the BHJ structure in OSCs is thermodynamically vulnerable to heat because of the fullerene aggregation,[15,33] we found that

introducing AZO can hinder the OSCs' degree of thermal degradation. This result was mainly attributed to the passivation of oxygen-deficient defects on the AZO surface and the reduced space-charge limited current (SCLC) region. The light intensity (P_{light})-dependent open-circuit voltage (V_{OC}) was measured and x-ray photoelectron spectroscopy (XPS) was conducted, which revealed a positive correlation between the oxygen-deficient defects and degradation. In addition, the photocurrent density (J_{ph}), as a function of effective voltage (V_{eff}), was analyzed to determine the correlation between the electrical properties and device stability.

The detailed experimental procedures are described as follows: the structure of OSCs used in the experiment was ITO\ETL\poly[4,8-bis(5–(2-ethylhexyl)thiophen-2-yl)benzo[1,2-b;4,5-b']dithiophene-2,6-diyl-alt-(4–(2-ethylhexyl)-3-fluorothieno[3,4-b]thiophene-)-2-carboxylate-2–6-diyl)] (PTB7-th):[6,6]-phenyl C71 butyric acid methyl ester ($PC_{70}BM$)\MoO_3\Al. In brief, a glass substrate with a patterned indium tin oxide (ITO) was prepared after sequentially washing with acetone, isopropyl alcohol (IPA), and de-ionized water (DI). Then, ETLs, including AZO and ZnO solutions, were spin-coated on the patterned ITO. The ZnO solution was prepared as described in a previous article.[34] In brief, zinc acetate dihydrate (1 g) was dissolved in 2-methoxy ethanol (10 ml) with a dropwise addition of ethanolamine (0.276 ml). In regard to the AZO solution, aluminum nitrate nonahydrate (0.3418 g) was added to a solution with the above composition and with the same stabilizer amount. The photoactive layer solution was prepared by dissolving PTB7-th:$PC_{70}BM$ (1:2 ratio by weight) in 1,2-dichloro benzene (1,2-DCB) to a total concentration of 36 mg ml^{-1}. The solution was stirred at 70 °C overnight with the addition of 1,8-diiodooctane (DIO) (25 μl) immediately before spin-coating. The photoactive layer solution was spin-coated above the ETL at 1000 rpm for 60 s, followed by storage in high vacuum (10^{-6} Torr) overnight. Then, MoO_3 (10 nm) and Al (100 nm) were sequentially thermally evaporated. The current density–voltage (J–V) characteristics, including the short circuit current (J_{SC}), V_{OC}, fill factor (FF), and PCE, were measured using a Keithley 237 source measurement unit with an AM 1.5G solar simulator (Newport, 91160A). The incident photon-to-electron conversion efficiency (IPCE) was characterized using a measurement system (Newport, QEPVSI-B). XPS (Kratos. Inc, AXIS-HSi) and ultraviolet photon spectroscopy (UPS) (Kratos. Inc., AXIS-NOVA) were performed for analyzing the film. For precise XPS and UPS analyses, the samples were thermally annealed in a separate vacuum chamber and transferred to the measurement systems by a low-vacuum desiccator to exclude contamination issues by carbon and oxygen. The thermal stability of devices was measured using a temperature controller (Lake Shore Cryotronics model 331). The devices were kept in a vacuum chamber at 85 °C.

In Fig. 1, the J–V characteristics and photovoltaic parameters of the AZO and ZnO devices are compared for the pristine and aged samples. Hereafter, we name devices with a specific ETL as an "ETL device." For example, a device with AZO is called an AZO device. The performance of the AZO device (J_{SC} = 15.34 mA cm^{-2}, V_{OC} = 0.82 V, FF = 0.69, and PCE = 8.65%) shows a comparable increase compared to the ZnO device (J_{SC} = 15.04 mA cm^{-2}, V_{OC} = 0.81 V, FF = 0.68, and PCE = 8.33%). As reported previously, the enhanced performance of the AZO device can be attributed to the large number of density of states (DOS) at the conduction band, consequently leading to a low resistivity.[35] Furthermore, AZO has a wider optical bandgap (E_g) than

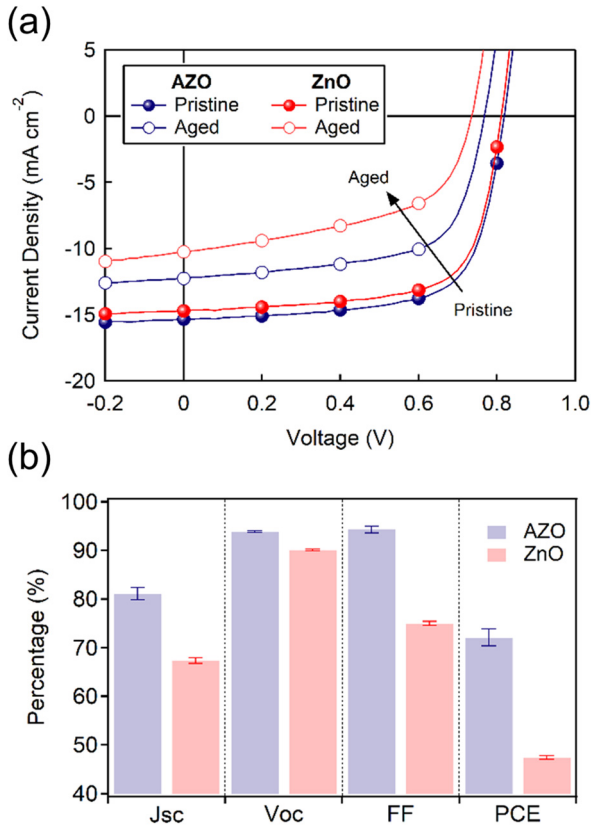

FIG. 1. (a) J–V characteristics and (b) normalized values of the photovoltaic parameters of AZO- and ZnO-adopted OSCs after thermal degradation at 85 °C.

ZnO due to the Burstein–Moss shift, thereby leading to an increased absorption of light in the ultraviolet (UV) region and an improved J_{SC} [Fig. 1(a)].[36] To reveal the effect of the interfacial layer on the device stability, samples with the AZO and ZnO ETLs were kept at 85 °C in a dark environment, which parallels the widely adopted stability testing protocol.[37] The photovoltaic parameters (J_{SC}, V_{OC}, FF, and PCE) are higher for the AZO device than for the ZnO device after the thermal aging test (Table I). After applying 6 h of thermal annealing, the parameters of the AZO device decrease to J_{SC} = 12.25 mA cm^{-2}, V_{OC} = 0.77 V, FF = 0.64, and PCE = 6.06%, while the parameters of the ZnO device decrease to J_{SC} = 10.25 mA cm^{-2}, V_{OC} = 0.74 V, FF = 0.53, and PCE = 3.98%.

In Fig. 1(b), the alteration of the photovoltaic parameters of both devices is compared simultaneously. While V_{OC} shows a relatively small difference, J_{SC} and FF show a considerable discrepancy depending on the ETL; those of the AZO device appear to be more stable against heat in contrast to the ZnO device. In particular, the FF of the AZO device maintains 93% of its initial value even after the entire degradation process (6 h). In comparison, the FF of the ZnO device decreases to 78% of its initial value. Since J_{SC} and FF are sensitively determined by the interaction between the charge extraction and recombination,[38] it is speculated that these deviations are ascribed to the different alterations of the interface between the photoactive layer and the respective ETLs. However, in regard to the V_{OC}, both the AZO and ZnO devices show

TABLE I. Performance parameters[a,b] of the AZO- and ZnO-adopted OSCs after thermal degradation.

	AZO sol–gel		ZnO sol–gel	
…	Pristine	Aged	Pristine	Aged
J_{SC} (mA cm^{-2})	15.05 ± 0.25 (15.34)	12.45 ± 0.19 (12.25)	14.74 ± 0.19 (15.04)	10.14 ± 0.09 (10.25)
V_{OC} (V)	0.82 ± 0.00 (0.82)	0.77 ± 0.00 (0.77)	0.81 ± 0.00 (0.81)	0.74 ± 0.00 (0.74)
FF	0.68 ± 0.01 (0.69)	0.65 ± 0.01 (0.64)	0.69 ± 0.01 (0.68)	0.53 ± 0.00 (0.53)
PCE (%)	8.35 ± 0.21 (8.65)	6.23 ± 0.15 (6.06)	8.18 ± 0.13 (8.33)	3.95 ± 0.03 (3.98)

[a]Average and standard deviation calculated on 6 independent data.
[b]The numbers in parentheses are the maximum value of each condition.

relatively stabilized values, maintaining 94 and 91% of their initial values after 6 h of thermal degradation. The comparatively low degradation of V_{OC} is attributed to the consistent Fermi level of each ETL after thermal annealing, which will be discussed in a later paragraph, and the device structure with of MoO_3\Al, which is known to have a stable V_{OC} after thermal degradation.[28] Consequently, the PCE, a combined index of J_{SC}, V_{OC}, and FF, is more stable for the AZO device than for the ZnO device, retaining 70 and 48% of their initial efficiencies, respectively, after the 6-h aging test. To reveal the fundamental reason for the different J_{SC} and FF alterations, further in-depth analyses were conducted.

$$V_{OC} = \frac{E_g}{q} - \frac{nkT}{q}\ln\left[\frac{(1-P_D)\gamma N_C^2}{P_D G}\right]. \quad (1)$$

The P_{light}-dependent V_{OC} of devices with AZO and ZnO upon thermal degradation was measured to reveal the charge recombination alteration [Figs. 2(a) and 2(b)]. Briefly, the ratio of V_{OC} to the natural logarithm of P_{light} generally shows a linear equation.[39] In Eq. (1), E_g is the bandgap, q is the elementary charge, n is the ideality factor, k is the Boltzmann constant, T is the temperature in Kelvin, P_D is the dissociation probability, γ is the Langevin recombination constant, N_C is the effective density of states, and G is the generation rate. The ideality factor (n) equals 1 when bimolecular recombination is the only recombination mechanism observed. However, after the device experiences severe damage by trap-assisted recombination, the ideality factor (n) starts to increase, of which the maximum is 2. The slope of AZO increases from 0.98 to 1.14, but that of ZnO increases from 1.00 to 1.32. Thus, it can be interpreted that more trap-assisted recombination occurs in the ZnO device compared to the AZO device. As a result, the recombination loss inside the ZnO device increases significantly, thereby resulting in a significantly reduced FF and J_{SC}. In contrast, the carrier recombination behavior is less affected in the AZO device, which is in line with the suppression of premature degradation.

Furthermore, qualitative analyses of oxygen were conducted using XPS measurements (Fig. 3). The low binding energy spectrum of the O 1s core, denoted as O_A, at 530.0 eV originates from the O^{2-} ions in the wurtzite structure of the hexagonal Zn^{2+} array (Zn-O bond). In contrast, the high binding energy spectrum, denoted as O_B, at 531.5 eV originates from the oxygen-deficient defects (zinc hydroxide) in the ZnO matrix.[40–45] The ratio of O_B to O_A is positively related to the oxygen-deficient defects on the surface, which is known to decrease charge extraction and deteriorates the device performance. Chen *et al.* reported that the UVO treatment of ZnO passivates the oxygen-deficient defects and reduces the carrier recombination at the interface between the ZnO and the photoactive layer, which eventually enhances the OSC characteristics.[46] In addition, Lin *et al.* revealed that thermal (150 °C) and vacuum (10^{-6} Torr) post-treatments of the ZnO layer effectively reduced the oxygen-deficient defects, including zinc hydroxide, leading to an improved electron extraction in OSCs.[47]

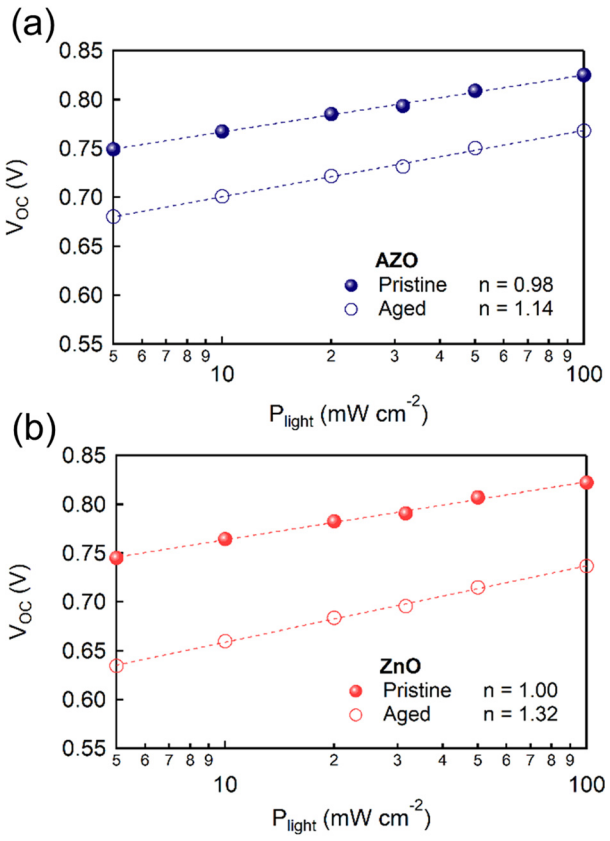

FIG. 2. P_{light}-dependent V_{OC} of the (a) AZO and (b) ZnO devices after thermal degradation.

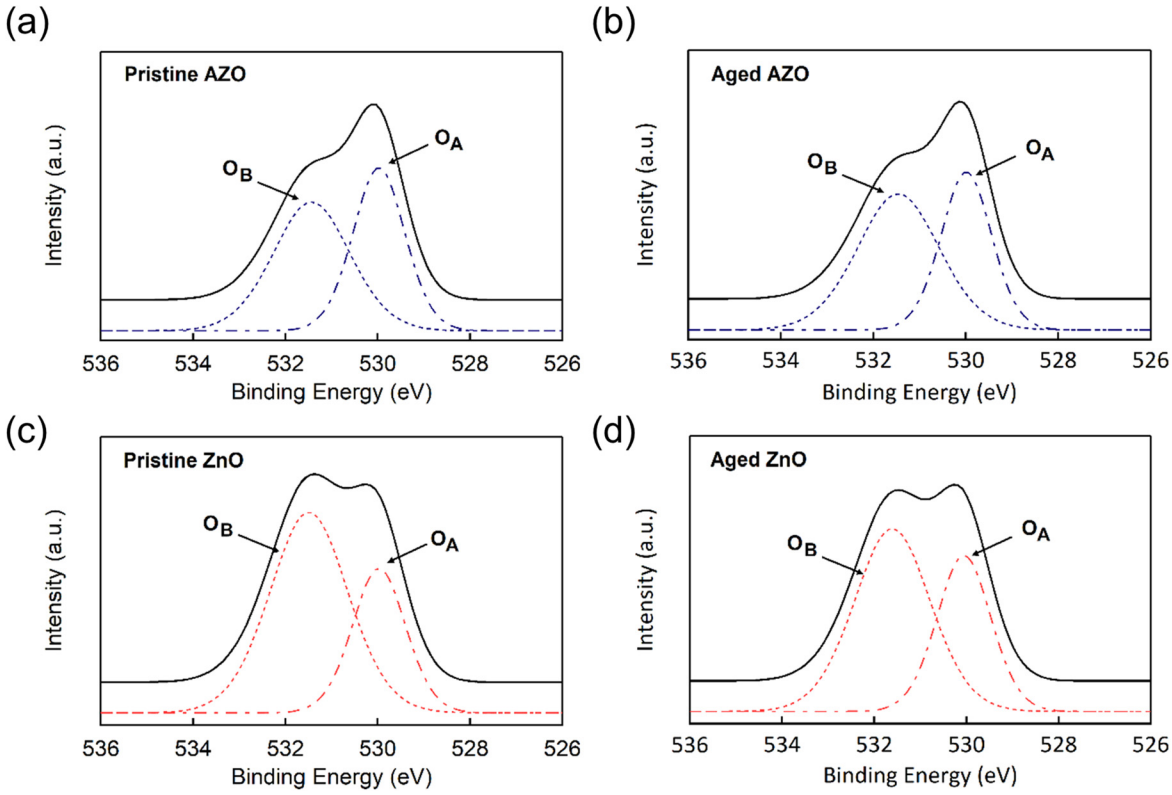

FIG. 3. Qualitative analyses of oxygen by the XPS measurements of the (a) and (b) AZO and (c) and (d) ZnO films.

Similarly, we also reported that oxygen-deficient defects on the surface of an ETL sensitively affect light-induced aging by increasing charge recombination and broadening the density of states.[48] In line with the previous studies, the ratios of O_B to O_A positively correlate with the thermal degradation tendency of OSCs depending on the ETLs (Fig. 3). Specifically, the ratio of O_B to O_A is larger for pristine ZnO than for pristine AZO, indicating that more oxygen-deficient defects are involved in the ZnO surface, resulting in relatively low stability. Upon thermal aging, the ZnO film shows a slight decrease in the ratio of O_B to O_A, which is attributed to the desorption of the by-product by the thermal annealing effect.[40] Nevertheless, the overall tendency of the ratio of O_B to O_A shows a similar trend regardless of thermal aging. Therefore, it can be interpreted that the initially formed oxygen-deficient defects on the surface dominate the device's thermal stability, while there are no significant variations in the layer itself. However, the difference in the density of oxygen-deficient defects between AZO and ZnO is mainly attributed to the passivated surface of AZO with Al^{3+} ions, which results in a significant decrease in oxygen-deficient defects.[49]

Considering the P_{light}-dependent V_{OC} (Fig. 2) and XPS results (Fig. 3), one reason for the difference in stability between AZO and ZnO originates from their surface properties in regard to an oxygen deficiency. However, considering that the improved PCE of AZO, compared to ZnO, is usually attributed to the surface passivation and improved charge transport,[35] an analysis regarding the charge transport property is required.

$$J_{ph} = q\left(\frac{9\varepsilon_0\varepsilon_r\mu}{8q}\right)^{1/4} G^{3/4} V_{eff}{}^{1/2}. \quad (2)$$

It is widely known that analyzing the dependence of the photocurrent (J_{ph}) on the effective voltage (V_{eff}), where V_{eff} is the bias voltage (V_{bias}) subtracted from the built-in voltage (V_0), provides insight into the carrier transport inside the OSC. Depending on the relationship, the carrier transport inside the OSC can be categorized into three different mechanisms: (1) Ohmic, (2) SCLC, and (3) saturation regions.[50,51] The linear dependence of J_{ph} on V_{eff} implies an Ohmic conduction region. After that, a saturation region follows, in which the J_{ph} and V_{eff} are irrelevant with the absence of the SCLC region. However, in the presence of the SCLC region, J_{ph} shows a square root dependence on V_{eff}. The SCLC region originates from the asymmetric mobility in electrons and holes, which leads to a high recombination rate or a low fill factor.[50,52] In Fig. 4, the J–V characteristics in terms of J_{ph} and V_{eff} are plotted. In regard to the both pristine and aged AZO devices, J_{ph} shows a linear region in the low V_{eff} region, which is directly followed by a saturation region after $V_{eff} = 0.5$ V. This result indicates that the AZO-adopted devices are not under the influence of the SCLC region, which is in line with its superior charge transport property. Contrary to the AZO case, the aged ZnO device shows different results, including the subsidiary SCLC region with an exponent close to 0.460 from $V_{eff} = 0.6$–0.8 V. Considering the identical saturated J_{ph} of the AZO device regardless of thermal degradation, it can be assumed that the generation rate (G) rarely changed

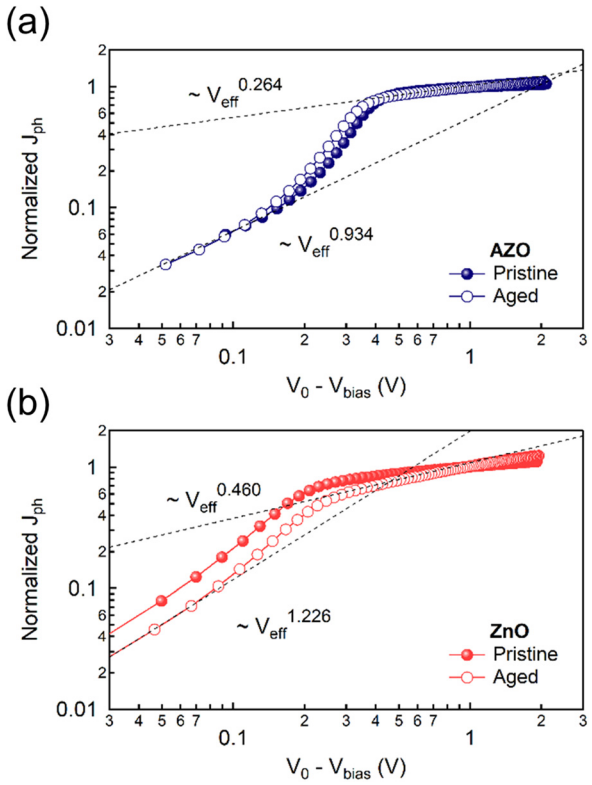

FIG. 4. J_{ph} as a function of $V_0 - V_{bias}$ of the (a) AZO- and (b) ZnO-adopted OSCs before and after thermal degradation.

for both the AZO and the ZnO devices as they share the same photoactive layer structure. In other words, it can be interpreted that the ZnO device's electron mobility (μ) decreased 3.22-fold smaller by comparing the different J_{ph} after thermal degradation, while that of the AZO device showed ignorable variation. Therefore, the aged ZnO device is unfavorable due to its inferior charge transport properties, which results in additional SCLC formation. It is commonly shown that the FF is most sensitively influenced by the charge transport property, among other factors.[53] The AZO device retains 94% of its initial FF, decreasing from 0.69 to 0.65, but the ZnO device retains only 77%, decreasing from 0.69 to 0.53 (Table I). Thus, it can be concluded that the different degrees of the SCLC region significantly contribute to the varying levels of thermal degradation in the OSCs.

To obtain further insight into the film alterations due to thermal degradation, additional measurements regarding energy level shifts were conducted. We focused on the degradation possibility due to the energy level shift after thermal degradation for the AZO and ZnO films annealed at 85 °C (Fig. 5). In particular, the work function (ϕ) of ZnO showed an insignificant shift from 4.0 eV, while that of AZO showed a relatively large change from 3.7 to 3.8 eV after thermal degradation. According to several former articles, the vacuum-annealing upon AZO releases the oxygen from the film and increases the oxygen vacancies or deficient states,[54,55] which consequently enlarges the work function.[56] However, the difference of work function between the AZO and ZnO films decreased after thermal degradation, which interprets that the energy level shifts cannot be the reason for the difference in thermal stability behavior. Based on the film analysis, we assume that the characteristic thermal degradation of each device is not from the ETL itself but from the interface between the ETL and photoactive layer.

In conclusion, we discussed the decreased thermal degradation of OSCs by introducing AZO as an ETL instead of ZnO. Under thermal stress (85 °C) without light irradiation, the AZO device is much more stable than the ZnO device, as proven by the different PCE degradation rates (AZO device: 70% and ZnO device: 48%). This difference in stability is attributed to the dissimilar recombination and charge transport properties at the interface between the ETL and photoactive layer, which is confirmed through the ideality factor (n) extrapolated from the variation in V_{OC} against P_{light}, the qualitative analysis by XPS, and J_{ph} as a function of V_{eff}. We believe that the proposed device architecture with enhanced thermal stability will provide further insight into overcoming the degradation issues of OSCs.

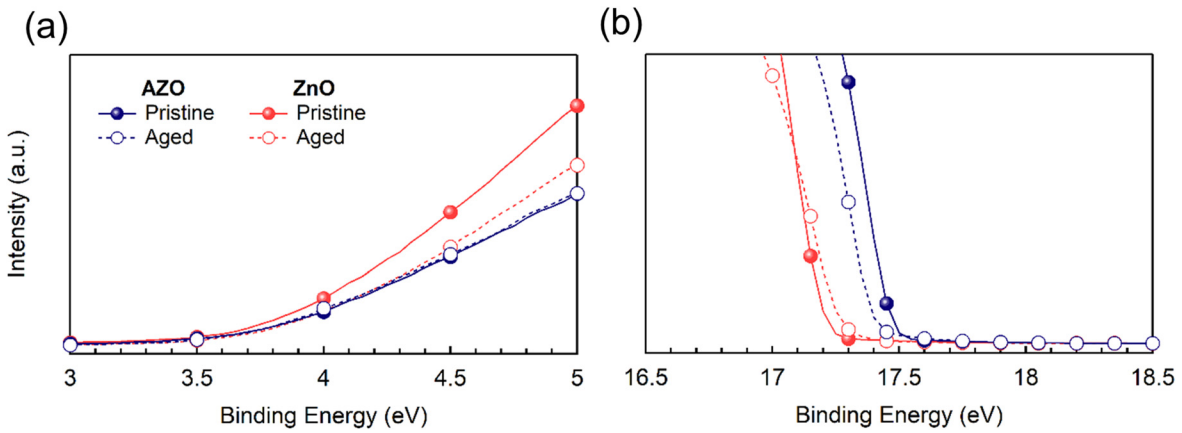

FIG. 5. (a) Valence band edge and (b) secondary electron cutoff of the AZO and ZnO films after thermal degradation, as measured by UPS.

See the supplementary material for the IPCE, P_{light}-dependent J_{SC}, and UPS variation of various devices and samples upon thermal degradation.

AUTHORS' CONTRIBUTIONS

J.K. and Y.L. contributed equally to this work.

This work was supported by the Basic Science Research Program (No. NRF-2019R1F1A1057693) through the National Research Foundation of Korea grant, which is funded by the Ministry of Science and ICT.

DATA AVAILABILITY

The data that support the findings of this study are available from the corresponding author upon reasonable request.

REFERENCES

[1]D. Gielen, F. Boshell, D. Saygin, M. D. Bazilian, N. Wagner, and R. Gorini, Energy Strategy Rev. **24**, 38 (2019).
[2]D. Vak, S.-S. Kim, J. Jo, S.-H. Oh, S.-I. Na, J. Kim, and D.-Y. Kim, Appl. Phys. Lett. **91**, 081102 (2007).
[3]S. B. Darling and F. You, RSC Adv. **3**, 17633 (2013).
[4]M. Kaltenbrunner, M. S. White, E. D. Głowacki, T. Sekitani, T. Someya, N. S. Sariciftci, and S. Bauer, Nat. Commun. **3**, 770 (2012).
[5]M. W. Rowell, M. A. Topinka, M. D. McGehee, H.-J. Prall, G. Dennler, N. S. Sariciftci, L. Hu, and G. Gruner, Appl. Phys. Lett. **88**, 233506 (2006).
[6]T. F. O'Connor, A. V. Zaretski, S. Savagatrup, A. D. Printz, C. D. Wilkes, M. I. Diaz, E. J. Sawyer, and D. J. Lipomi, Sol. Energy Mater. Sol. Cells **144**, 438 (2016).
[7]S. Berny, N. Blouin, A. Distler, H.-J. Egelhaaf, M. Krompiec, A. Lohr, O. R. Lozman, G. E. Morse, L. Nanson, A. Pron, T. Sauermann, N. Seidler, S. Tierney, P. Tiwana, M. Wagner, and H. Wilson, Adv. Sci. **3**, 1500342 (2016).
[8]S. Liu, J. Yuan, W. Deng, M. Luo, Y. Xie, Q. Liang, Y. Zou, Z. He, H. Wu, and Y. Cao, Nat. Photonics **14**, 300 (2020).
[9]Q. Li, Y. Sun, C. Yang, K. Liu, M. R. Islam, L. Li, Z. Wang, and S. Qu, Sci. Bull. **65**, 747 (2020).
[10]H. Feng, Y.-Q.-Q. Yi, X. Ke, J. Yan, Y. Zhang, X. Wan, C. Li, N. Zheng, Z. Xie, and Y. Chen, Adv. Energy Mater. **9**, 1803541 (2019).
[11]S. A. Gevorgyan, M. V. Madsen, B. Roth, M. Corazza, M. Hösel, R. R. Søndergaard, M. Jørgensen, and F. C. Krebs, Adv. Energy Mater. **6**, 1501208 (2016).
[12]L. Duan and A. Uddin, Adv. Sci. **7**, 1903259 (2020).
[13]G. Yu, J. Gao, J. C. Hummelen, F. Wudl, and A. J. Heeger, Science **270**, 1789 (1995).
[14]F. Piersimoni, G. Degutis, S. Bertho, K. Vandewal, D. Spoltore, T. Vangerven, J. Drijkoningen, M. K. Van Bael, A. Hardy, J. D'Haen, W. Maes, D. Vanderzande, M. Nesladek, and J. Manca, J. Polym. Sci., Part B **51**, 1209 (2013).
[15]P. Cheng, C. Yan, Y. Wu, S. Dai, W. Ma, and X. Zhan, J. Mater. Chem. C **4**, 8086 (2016).
[16]Y.-J. Hsieh, Y.-C. Huang, W.-S. Liu, Y.-A. Su, C.-S. Tsao, S.-P. Rwei, and L. Wang, ACS Appl. Mater. Interfaces **9**, 14808 (2017).
[17]Y. Wang, W. Lan, N. Li, Z. Lan, Z. Li, J. Jia, and F. Zhu, Adv. Energy Mater. **9**, 1900157 (2019).
[18]S. Park, H. Ahn, J-y Kim, J. B. Park, J. Kim, S. H. Im, and H. J. Son, ACS Energy Lett. **5**, 170 (2020).
[19]S. Badgujar, C. E. Song, S. Oh, W. S. Shin, S.-J. Moon, J.-C. Lee, I. H. Jung, and S. K. Lee, J. Mater. Chem. A **4**, 16335 (2016).
[20]R. Yu, H. Yao, L. Hong, Y. Qin, J. Zhu, Y. Cui, S. Li, and J. Hou, Nat. Commun. **9**, 4645 (2018).
[21]W. Yang, Z. Luo, R. Sun, J. Guo, T. Wang, Y. Wu, W. Wang, J. Guo, Q. Wu, M. Shi, H. Li, C. Yang, and J. Min, Nat. Commun. **11**, 1218 (2020).
[22]D. Yang, F. C. Löhrer, V. Körstgens, A. Schreiber, S. Bernstorff, J. M. Buriak, and P. Müller-Buschbaum, ACS Energy Lett. **4**, 464 (2019).
[23]G. Griffini, J. D. Douglas, C. Piliego, T. W. Holcombe, S. Turri, J. M. J. Fréchet, and J. L. Mynar, Adv. Mater. **23**, 1660 (2011).
[24]N. Gasparini, S. H. K. Paleti, J. Bertrandie, G. Cai, G. Zhang, A. Wadsworth, X. Lu, H.-L. Yip, I. McCulloch, and D. Baran, ACS Energy Lett. **5**, 1371 (2020).
[25]D. Gao, J. Hollinger, and D. S. Seferos, ACS Nano **6**, 7114 (2012).
[26]I. T. Sachs-Quintana, T. Heumüller, W. R. Mateker, D. E. Orozco, R. Cheacharoen, S. Sweetnam, C. J. Brabec, and M. D. McGehee, Adv. Funct. Mater. **24**, 3978 (2014).
[27]F. Hermerschmidt, A. Savva, E. Georgiou, S. M. Tuladhar, J. R. Durrant, I. McCulloch, D. D. C. Bradley, C. J. Brabec, J. Nelson, and S. A. Choulis, ACS Appl. Mater. Interfaces **9**, 14136 (2017).
[28]W. Greenbank, L. Hirsch, G. Wantz, and S. Chambon, Appl. Phys. Lett. **107**, 263301 (2015).
[29]X. Zhao, H. Shen, Y. Zhang, X. Li, X. Zhao, M. Tai, J. Li, J. Li, X. Li, and H. Lin, ACS Appl. Mater. Interfaces **8**, 7826 (2016).
[30]S. Trost, K. Zilberberg, A. Behrendt, A. Polywka, P. Görrn, P. Reckers, J. Maibach, T. Mayer, and T. Riedl, Adv. Energy Mater. **3**, 1437 (2013).
[31]Z. Kam, X. Wang, J. Zhang, and J. Wu, ACS Appl. Mater. Interfaces **7**, 1608 (2015).
[32]M. Prosa, M. Tessarolo, M. Bolognesi, O. Margeat, D. Gedefaw, M. Gaceur, C. Videlot-Ackermann, M. R. Andersson, M. Muccini, M. Seri, and J. Ackermann, ACS Appl. Mater. Interfaces **8**, 1635 (2016).
[33]C. H. Yi Ho, H. Cao, Y. Lu, T.-K. Lau, S. H. Cheung, H.-W. Li, H. Yin, K. L. Chiu, L.-K. Ma, Y. Cheng, S.-W. Tsang, X. Lu, S. K. So, and B. S. Ong, J. Mater. Chem. A **5**, 23662 (2017).
[34]Y. Sun, J. H. Seo, C. J. Takacs, J. Seifter, and A. J. Heeger, Adv. Mater. **23**, 1679 (2011).
[35]J. Y. Kim, E. Cho, J. Kim, H. Shin, J. Roh, M. Thambidurai, C-m Kang, H.-J. Song, S. Kim, H. Kim, and C. Lee, Opt. Express **23**, A1334 (2015).
[36]Y.-S. Kim and W.-P. Tai, Appl. Surf. Sci. **253**, 4911 (2007).
[37]M. O. Reese, S. A. Gevorgyan, M. Jørgensen, E. Bundgaard, S. R. Kurtz, D. S. Ginley, D. C. Olson, M. T. Lloyd, P. Morvillo, E. A. Katz, A. Elschner, O. Haillant, T. R. Currier, V. Shrotriya, M. Hermenau, M. Riede, K. R. Kirov, G. Trimmel, T. Rath, O. Inganäs, F. Zhang, M. Andersson, K. Tvingstedt, M. Lira-Cantu, D. Laird, C. McGuiness, S. Gowrisanker, M. Pannone, M. Xiao, J. Hauch, R. Steim, D. M. DeLongchamp, R. Rösch, H. Hoppe, N. Espinosa, A. Urbina, G. Yaman-Uzunoglu, J.-B. Bonekamp, A. J. J. M. van Breemen, C. Girotto, E. Voroshazi, and F. C. Krebs, Sol. Energy Mater. Sol. Cells **95**, 1253 (2011).
[38]Z. He, C. Zhong, X. Huang, W.-Y. Wong, H. Wu, L. Chen, S. Su, and Y. Cao, Adv. Mater. **23**, 4636 (2011).
[39]A. K. K. Kyaw, D. H. Wang, V. Gupta, W. L. Leong, L. Ke, G. C. Bazan, and A. J. Heeger, ACS Nano **7**, 4569 (2013).
[40]A. G. Marrani, F. Caprioli, A. Boccia, R. Zanoni, and F. Decker, J. Solid State Electrochem. **18**, 505 (2014).
[41]L.-J. Meng, C. P. Moreira de Sá, and M. P. dos Santos, Appl. Surf. Sci. **78**, 57 (1994).
[42]M. Valtiner, S. Borodin, and G. Grundmeier, Phys. Chem. Chem. Phys. **9**, 2406 (2007).
[43]L. L. Yang, Q. X. Zhao, M. Willander, X. J. Liu, M. Fahlman, and J. H. Yang, Appl. Surf. Sci. **256**, 3592 (2010).
[44]U. Meier and C. Pettenkofer, Appl. Surf. Sci. **252**, 1139 (2005).
[45]S. Sepulveda-Guzman, B. Reeja-Jayan, E. de la Rosa, A. Torres-Castro, V. Gonzalez-Gonzalez, and M. Jose-Yacaman, Mater. Chem. Phys. **115**, 172 (2009).
[46]S. Chen, C. E. Small, C. M. Amb, J. Subbiah, T.-H. Lai, S.-W. Tsang, J. R. Manders, J. R. Reynolds, and F. So, Adv. Energy Mater. **2**, 1333 (2012).
[47]Z. Lin, J. Chang, C. Jiang, J. Zhang, J. Wu, and C. Zhu, RSC Adv. **4**, 6646 (2014).
[48]J. Kim, H. Jung, J. Song, K. Kim, and C. Lee, ACS Appl. Mater. Interfaces **9**, 24052 (2017).
[49]S.-Y. Kuo, W.-C. Chen, F.-I. Lai, C.-P. Cheng, H.-C. Kuo, S.-C. Wang, and W.-F. Hsieh, J. Cryst. Growth **287**, 78 (2006).
[50]V. D. Mihailetchi, J. Wildeman, and P. W. M. Blom, Phys. Rev. Lett. **94**, 126602 (2005).

[51]W. E. I. Sha, X. Li, and W. C. H. Choy, Sci. Rep. **4**, 6236 (2014).
[52]J. D. Morris, T. L. Atallah, C. J. Lombardo, H. Park, A. Dodabalapur, and X.-Y. Zhu, Appl. Phys. Lett. **102**, 033301 (2013).
[53]B. Qi and J. Wang, Phys. Chem. Chem. Phys. **15**, 8972 (2013).
[54]B. Zhu, K. Lü, J. Wang, T. Li, J. Wu, D. Zeng, and C. Xie, J. Vac. Sci. Technol., A **31**, 061513 (2013).
[55]B. P. Shantheyanda, V. O. Todi, K. B. Sundaram, A. Vijayakumar, and I. Oladeji, J. Vac. Sci. Technol., A **29**, 051514 (2011).
[56]X. Jiang, F. L. Wong, M. K. Fung, and S. T. Lee, Appl. Phys. Lett. **83**, 1875 (2003).